

# APPLICATION OF ELECTRICAL CAPACITANCE TOMOGRAPHY FOR DENSE CROSS-SECTIONAL PARTICLE MIGRATION IN A MICROCHANNEL

## Article history

Received

28 June 2015

Received in revised form

1 September 2015

Accepted

15 October 2015

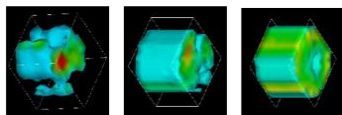
Nur Tantiyani Ali Othman<sup>a\*</sup>, Masahiro Takeji<sup>b</sup>

\*Corresponding author  
tantiyani@ukm.edu.my

<sup>a</sup>Department of Chemical and Process Engineering, Faculty of Engineering and Built Environment, Universiti Kebangsaan Malaysia, 43600 UKM Bangi, Selangor, Malaysia

<sup>b</sup>Department of Mechanical Engineering, Faculty of Engineering, Chiba University, Japan

## Graphical abstract



## Abstract

In microfluidic applications, in order to produce the high yield of desired product, the study of particle migration is very important to enhancement and increases the efficiency of positioning and sorting process. One of an effective and robust method for visualization imaging, passively positioning and sorting microparticles and cells without the assistance of sheath fluid is electrical capacitance. In this study, to study the behavior of particle migration, a fine particle concentration in a cross-sectional microchannel is determined for the high dense initial particle concentrations ( $\xi=10.0\%$ ) and small particle diameters ( $d_p=2.1\ \mu\text{m}$ ) by using a high speed multiplexer and 12 multi-layer electrical capacitance tomography (ECT) sensing to discuss the stream migration along five cross-sections. The polystyrene particles as solid phase and non-conductive deionized water as a liquid phase are non-uniformly injected into the inlets microchannel. From the electrical capacitance distribution, the tomography images that show the equilibrium particle migration is reconstructed by used the Tikhonov regularization method. It has been observed that the particle concentration at the wall vicinity area is increased as  $\xi$  and  $d_p$  are increased while the particle concentration at the center area is decreased. It shows the particles are moved away from the center towards wall vicinity area and particles migrated towards the wall increased in the outlet area as the particles move along the cross-sectional microchannel. The experimental result is verified with the COMSOL simulation.

**Keywords:** Capacitance cross-sectional microchannel, multi-layer electrodes, particle concentration distribution, stream transitional migration, tomography

© 2015 Penerbit UTM Press. All rights reserved

## 1.0 INTRODUCTION

Particle migration is observed to occur regularly from large pipe to micro scale, particularly when suspending fluid is aqueous and thus of low viscosity. Generally, suspended particles are known to migrate in a pressure-driven flow at the finite-inertia conditions. This is called tubular a pinch phenomenon, successfully described by a theory for a point particle limit in the

channel and tube geometries [1]. Numerous studied on the particles migration in a large pipe scale are reported since early 1962. The particle migration effect was first observed by Segre and Silberberg [1] for dilute suspension flow ( $\xi \leq 1.0\%$ ) through pipe with Reynolds number ( $Re$ ) based on pipe width ( $D$ ) is in the interval from  $Re=2-700$ . They observed that the particles concentration is non-uniform with maximum concentration being at radial position  $0.6D$ ; from the

centerline. Since that, it has triggered a series of experiment and theoretical studies on the particles migration regarding in a tube, channel and Couette flow, and a laden with neutrally-buoyant particles and in circular pipes or planar channels [2-5].

As well as in a large pipe scale, researchers become attracted to investigate the particle migration in a micro scale size [6-10]. Normally, the length of the microchannel is in the order up to several hundred microns. Due to this condition, the transported particles are in order of less than 10  $\mu\text{m}$ . nowadays the particle migration in a micro scale can be utilized in a wide range of application such as for used of separating biological particles [11-12] or focusing on DNAs [13] in case of capillary-based microchannels with the dilute suspension flows. Consequently, the concept of the inertial particles migration in much type of the channel geometries and condition has been demonstrated [8-13]. Normally, to measure 3D inertial particle migration based on particles concentration in the microchannel, a micro particle image velocimetry ( $\mu\text{-PIV}$ ) is often used. The earliest experiments in the micro scale on the inertial particles migration within a vertical channel flow were performed by [14-15]. Their studied has showed particle migrates towards the wall vicinity area when it leads undisturbed flow and whereas in the case of less particle velocity, the migration in the opposite direction will take place [16-18]. In addition, the particles migration is reported to affect particles advection and particle interactions to move from center streamline toward wall vicinity area. It has been clarified through a number of previous experiments, particle migration strongly depends on the particle size; where the small particles tend to migrate toward wall vicinity area and cause a wall-peak particle distribution, whereas the larger particles tend to migrate toward center area and results in core-peak particle distribution. However, the  $\mu\text{-PIV}$  and typical optical visualization technique used in aforesaid previous studies is not applicable for a dense particle concentration ( $\xi \geq 1.0\%$ ) within a vertical cross-section since optical beam is scattered.

Thus, to overcome of this drawback, an electrical tomography measurement has a high possibility to measure a dense particle concentration in the particle-liquid phase flows. The multi-layer capacitance measurement; electrical capacitance tomography (ECT) is used to measure the particles concentration distribution at vertical cross-section based on the variation of the dielectric materials permittivity and capacitance distribution [19-20]. In the ECT technique, a sensor containing several electrodes is wrapped around circumference pipeline, and the capacitances distribution between the electrodes is measured. But, the prior typical wet process and conventional silicon etching process are available for hole type cross-section, which not available for the microchannel cross-section.

Thus, to resolve the problem of the conventional technique, in our previous studies, a microchannel with 12 multi-layer electrodes is successfully fabricated using micro-electro-mechanical-systems processes [21]. Our multi-layer microchannel has a possibility to visualize spatial transition of  $\xi=3.0\%$  particles in the vertical cross-section [22]. In addition, we investigated the effect of  $d_p=1.3, 1.5$  and  $2.1 \mu\text{m}$  on the particle migration in the microchannel by using the multi-layer capacitance technique [23-24]. Although the particles migration induced by inertial lift forces in the microchannel is a unique motion, however the detail studied is still required and not fully understood in terms of stream transitional as well as the dense initial particles concentrations.

Therefore, in this work, we focused on the stream cross-sectional migration as a parameter of the cross-sectional positions from the upstream; at  $z=0$  mm to the downstream cross-section; at  $z=20$  mm based on the multi-layer capacitance technique. The dense cross-sectional particle concentration;  $\xi=3.0-10.0\%$  and migration are determined and compared with the COMSOL simulation.

## 2.0 EXPERIMENTAL

### 2.1 Experimental Set-up

The experimental is set-up composed of two syringe pumps, microchannel, capacitance tomography and a computer. The syringe pumps (IC3100 [KDS100], KD Scientific, USA; dimension:  $23 \times 15 \times 12$  cm with a minimum step rate is 1 step per 30 s) are used to control the flow rate within 60 mL into the two inlets of the microchannel.

Microchannel of the microfluidic device is used in this study to investigate the behaviour of particle migration. The Y-shape microchannel has two inlets, two outlets and has five cross-sections embedding with 12 multi-layered electrodes. This microchannel embedded with a connector, sensor electrode and circuit board. The stable connection system is constructed in the microchannel in order to avoid unstable measurement conditions between the microchannel electrode tail and a capacitance measurement system and to consider the noise effect. The connection system is comprised of spring pins, top and bottom circuit boards, pin connectors and a central board [21]. The spring pin connects electrically the electrode tail and the circuit board. The detailed configuration of the microchannel used in this study is shown in Figure 1. Figure 1(a) shows the three-dimensional view of the microchannel and (b) shows the cross-sectional view of microchannel.

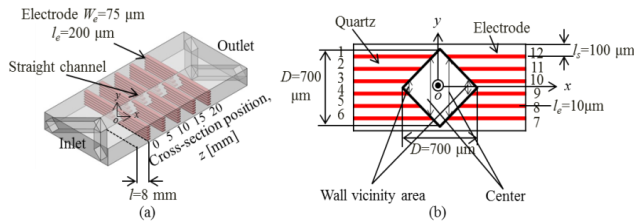


**Figure 1** Microchannel embedding 12 multi-layered electrodes with (a) Three-dimensional view and (b) Cross-sectional view

The microchannel has two inlets with angle  $\theta=30^\circ$  as shown in the left side of Figure 1(a) for flow injection, and two outlets with angle  $\theta=30^\circ$  as shown in the right side of Figure 1(a) for flow discharge. There is a straight diamond-shaped section in microchannel with length of  $z=20$  mm which is the main flow channel. This straight section of the microchannel has five cross-sections each separated by the distance of 5 mm. Each of these cross-sections has 12 multi layered electrodes. The cross-sectional dimensions i.e. channel width is  $D=700$   $\mu\text{m}$ . The origin of the coordinate system  $x$ ,  $y$  and  $z$  is located at the center point of the diamond shape cross-section ( $x$ - $y$  plane) and at the 8 mm distance ( $z$  direction) from the joint point of two inlets. The electrode's width  $w_e=75$   $\mu\text{m}$  and is along  $y$ -axis and the electrode's length is  $l_e=200$   $\mu\text{m}$  along  $x$ -axis. The electrode's material is platinum and the substrate's material is quartz glass. Substrate's length embedded with the electrode in the cross-sectional microchannel  $l_s=100$   $\mu\text{m}$  along the  $y$ -axis.

## 2.2 Experimental Conditions and Methods

The polystyrene particles suspended in the deionized water flow are injected through the inlets with pressure difference driven by the syringe pump at the controlled flow rate  $Q=4.9 \times 10^{-4}$   $\text{m}^3\text{s}^{-1}$ . The mean flow velocity calculated from  $Q$  is  $u=2.0 \times 10^{-3}$   $\text{ms}^{-1}$ , corresponds to the Poiseuille flow region at the flow Reynolds number  $Re=1000$  and particle  $Re_p=0.42$ . The relative permittivity of deionized water and polystyrene particle are  $\epsilon^{DW}=15.0$  and  $\epsilon^p=2.5$  respectively. The capacitances are measured between the electrode pairs under dense initial particle concentration  $\xi$ ;  $\xi=10.0$  v/v % and  $d_p=2.1$   $\mu\text{m}$  at the five cross-sections.

The electrical capacitance tomography (ECT) unit contains necessary AC bridge circuitry to measure the capacitance on the basis of the signals received from the microchannel electrode tails. The measurement signal is set to the ac voltage; 4.5 V at frequency of  $f=12.5$  MHz. Time required to take the one measurement between two unearthed electrodes is 25  $\mu\text{s}$ . We have employed 12 set of unearthed electrodes to measure the capacitance values in one cross-section resulting to 300  $\mu\text{s}$  for a complete set of measurement of a cross-section. Also, it is possible to measure the capacitance changes between two unearthed electrodes of the order of 0.01 fF in the

presence of stray capacitance to earth of 200 pF at a rate of 40,000 measurements per second [18]. Then, measured capacitance data is fed to the computer.

## 2.3 Image Reconstruction for ECT in Microchannel

The goal of image reconstruction in ECT is to compute a tomogram representing the electrical capacitance distribution of materials flowing within some column from voltages measured at the periphery of the sensor in response to the injected electrical current and voltage. To reconstruct the particle-liquid phase flow image for ECT in the microchannel, forward problem and inverse problem have to be solved. Knowing the capacitance distribution,  $C$  and given current injection, the problem of finding the electrical potential  $V$  inside or on the boundary of the microchannel between electrode pairs is called the forward problem.

Using finite element methods (FEM),  $\Delta C$  can be subdivided into  $n$  discrete values. Every discrete value corresponds to one pixel of the image reconstructed. Both direct and iterative algorithms can be formulated using different approximations, such like linear back-projection (LBP), Landweber method, Newton-Raphson method (NRM), and Tikhonov regularization method. In our experiment, we use the Tikhonov regularization method as the tool for image reconstruction. The details procedure in the reconstruction image can be refer to [18].

## 3.0 RESULTS AND DISCUSSIONS

### 3.1 Image Reconstruction

The changes of the capacitance distribution ( $\Delta C$ ) in every cross-section are reconstructed based on the measured boundary voltages using iterated Tikhonov regularization algorithm. By choosing  $\alpha=0.01$ , and stopping parameter  $\beta$  not greater than 0.001 to facilitate the convergence of the non-linear inverse problem. In this case the 3D reconstructed images of the dielectric permittivity distribution based on the  $\Delta C$  in three cross-sections are shown as in Figure 2 as examples.

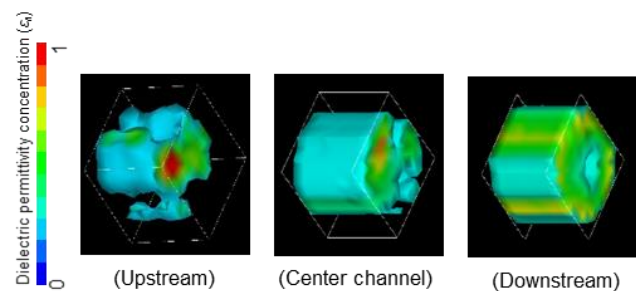


**Figure 2** 3D dielectric permittivity distribution on the three cross-sections that show particle concentration distribution

Figure 2 reveals the changes of dielectric permittivity distribution in three cross-sections in the microchannel. It shows along the flow direction from upstream cross-section; cross-section I to the downstream; cross-section V. Particle suspension and deionized water resolve into each other gradually except in the cross-section I, deionized water solution just meet each other. The result also reveals that under certain flow rate, micro particles have already dispersed evenly near cross-section V.

The reconstructed images of  $\Delta C$  on every cross-section show that the micro particles seem to have the tendency to disperse evenly within the liquid medium. This phenomenon agrees with the theory which claims that when two different phases are injected as the adjacent streams into one channel, one phase will often encapsulates the other phase. Although the test results is not very satisfactory, it agree basically with the real experiment condition which suggests that the ECT based measuring system can really work.

### 3.2 Cross-Sectional Particle Concentration

Some calculations are conducted to prove that the ECT can be successfully applied to the measurement of two-phase flows in microchannel. The cross-sectional particle concentration based on the capacitance distribution data measurement is calculated by using equation 1 [24].

$$(1-\phi)_{i-j} = \frac{\epsilon_{i-j}^P - \epsilon_{i-j}^{P0}}{\epsilon_{i-j}^{DW} - \epsilon_{i-j}^{P0}} \quad (1)$$

In the equation (1),  $\epsilon_{i-j}^{P0}$  is the permittivity between the electrodes  $i-j$  pair for particle suspended in deionized water in the calibration condition under a static condition to eliminate the stray capacitance with the superscript of  $P$  is for particle and  $DW$  is deionized water. From the equation (1), the averaged of the normalized particle concentrations distribution is determined. The cross-sectional particle concentration distribution is summarized as shown in Figure 3 at three cross-sections; cross-section I (upstream), III (center channel) and V (downstream). The vertical axis is the normalized particle concentration; range from 0.0-1.0; where 0.0 values means only single phase flow of deionized water and 1.0 value means all particles are dominant at the electrode pair area measurement. The horizontal axis is the position from center cross-sectional microchannel with  $R$  is the width of the cross-sectional microchannel.

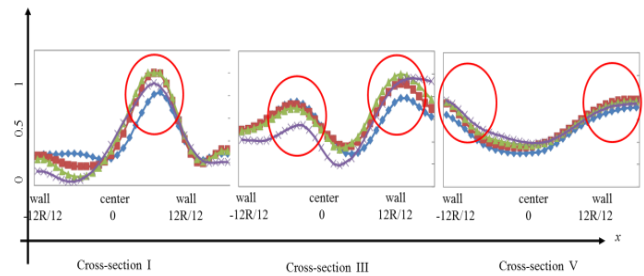


**Figure 3** Summarized of the normalized cross-sectional particle concentration distribution at the cross-section I, III and V

It is observed that at the upstream; cross-section I, the cross-sectional particle concentration distribution is much higher at the center than the wall vicinity area. While, at the cross-section III, the particle concentration at the center area of cross-sectional microchannel is slowly decreased to the area between the center and wall vicinity area. It shows the particle gradually mixed as particle moved from upstream cross-section; I to cross-section III. As a sequence, at the downstream cross-section V, the particle concentration distribution is higher near to the wall vicinity area and the lowest concentration indicated at the center area of cross-sectional microchannel. It clearly show particles tend to migrate towards near the wall area because the inertial lift force induced the interaction between particles that leads to the particle migration.

The parabolic laminar velocity also contributes to the shear-induced inertial lift force, drives particles away from the center toward the walls. As the particles migrated closer to walls, an asymmetric wake induced around the particle generates a wall-induced inertial lift force and drives particles away from the walls. From the parabolic velocity, a low gradient of particle velocity at center pushes particles toward walls, while a high gradient of particle velocity near the walls that drives particles back toward the center area of cross-sectional microchannel.

The calculation on the cross-sectional particle concentration shows at the upstream cross-section, particles are much more highly concentrated than at the electrode pairs near the center and has the lowest concentration near the walls. In contrast, particle concentration at the downstream cross-section is more highly concentrated near the channel walls. This is because at the upstream, the wall-induced lift force is dominant and pushes the particles toward center streamline. Moreover, due to wall-induced lift forces and gradient of velocity distribution, the particles moved and migrated to an equilibrium position. The balance between these forces finally results in the equilibrium of particle migration in the microchannel.

### 3.3 COMSOL Simulation

Additionally, the cross-sectional particle concentration and migration along cross-sections in the microchannel is simulated via COMSOL®. The microchannel design and simulation condition is same as in the experimental. The simulation result is expressed as shown in the Figure 4. At the cross-section I, particles marked as red is in the initial position of  $x < 0$  (inlet A) and particles marked as blue had initial position of  $x > 0$  (inlet B). As the particles started to follow the flow field and they begin to mix together in the microchannel flow. By the end of the microchannel outlet, the particles from two inlets have mixed completely. The blue and red mixed particles attract towards walls and some remains at center area.

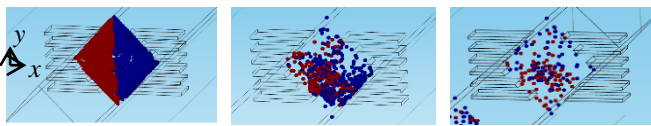


**Figure 4** Simulation of the particles concentration distributed at the cross-section I, III and V, respectively. The colour represents location of particle at its initial position

The particle migration in the microchannel can be conclude with the count number of particle simulation with the channel position along flow direction (z-axis). Figure 5 illustrates the histogram particle position that shows at the center channel the high concentration is indicated at the center and low at near the wall however, the number of the particle count increased at near the outlets that shows the particle migration is occurred as the particle moved from upstream to downstream cross-section in the microchannel.

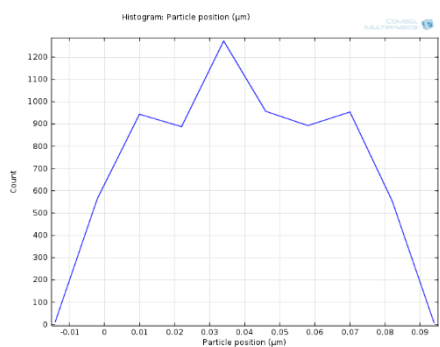


**Figure 5** Histogram of particle position in the cross-sectional microchannel

### 4.0 CONCLUSION

We use syringe injection method and ECT visualization to generate a stable liquid-solid two-phase flow in a novel experimental multi-layer microchannel for image reconstruction of the two phase flow. The image of particle-liquid phase flow is successfully reconstructed

by ECT system, the presence of the nonconductive microparticle in microfluids can alter the capacitance distribution inside the microchannel. Since all of the experimental results are based on non-conductive microparticle with same particle size and same flow rate, more detailed research should be done using particles of different physical property under other different test condition, meanwhile, the real time 3-dimension dynamic image reconstruction cannot be realized up to now due to the hardware setup restriction. Thus, in this study, the reconstruction tomography images of particles distribution are verified with the COMSOL simulation that shows the particle slightly moved and migrated from the center area of cross-sectional toward the wall vicinity area as the particle move along the five cross-sections.

### Acknowledgement

This study is supported by Adaptable and Seamless Technology Transfer Program through Target-driven R&D (A-Step) of Japan Science and Technology Agency (#AS2311054B).

### References

- [1] Segre, G., Silberberg, A. 1962. Behavior of Macroscopic Rigid Spheres in Poiseuille Flow: Part 1. Determination of Local Concentration by Statistical Analysis of Particle Passage through Crossed Light Beams. *Journal Fluid Mechanics*. 14: 115-135.
- [2] Jeffrey, C., Pearson, A. 1965. Particle Motion in Laminar Vertical Tube flow. *Journal Fluid Mechanics*. 22: 721-735.
- [3] Barry, J., Tallon, S. 1997. Concentration Variations within Pipe Cross-Sections in a Dilute Phase Pneumatic Conveying System. *IPENZ Transactions Journal*. 24: 1-11.
- [4] Asmolov, S. 1999. The Inertial Lift on a Spherical Particle in a Plane Poiseuille Flow at Large Channel Reynolds Number. *Journal Fluid Mechanics*. 381: 63-87.
- [5] Matas, P., Morris, F., Guazzelli, E. 2004. Inertial Migration of Rigid Spherical Particles in Poiseuille Flow. *Journal Fluid Mechanics*. 515: 171-195.
- [6] Ho, P., Leal, G. 1974. Inertial Migration of Rigid Spheres in Two-Dimensional Unidirectional Flows. *Journal Fluid Mechanics*. 65: 365-400.
- [7] Gwo-Bin, L., Chih-Chang, C., Sung-Bin H., Ruey-Jen, Y. 2006. The Hydrodynamic Focusing Effect inside Rectangular Microchannels. *Journal of Micromechanics and Microengineering*. 16: 1024.
- [8] Carlo, D., Irimia, D., Tompkins, G., Toner, M. 2007. Continuous Inertial Focusing, Ordering, and Separation of Particles in Microchannels. *Physics of Fluids*. 104: 18892-18897.
- [9] Asgar, A., Bhagal, S., Sathyakumar, S., Kuntaegowdanahalli, Papautsky, I. 2008. Enhanced Particle Filtration in Straight Microchannel Using Shear-Modulated Inertial Migration. *Physics of Fluids*. 20: 101702.
- [10] Choi, S., Seo, W., Lee J. 2011. Lateral and Cross-Lateral Focusing of Spherical Particles in A Square Microchannel. *The Royal Society of Chemistry*. 11: 460-465.
- [11] Ichiyanagi, M., Sasaki, S., Sato, Y., Hishida, K. 2009. Micro-PIV/LIF Measurements on Electrokinetically-Driven Flow in Surface Modified Microchannels. *Journal of Micromechanics and Microengineering*. 19: 1-9.
- [12] Curtin, M., Newport, T., Davies, R. 2006. Utilising  $\mu$ -PIV and Pressure Measurements to Determine the Viscosity of a DNA

- Solution in a Micro Channel. *Experimental Thermal and Fluid Science*. 30: 843-852.
- [13] Hoffmann, M., Schluter, M., Rabiger, N. 2006. Experimental Investigation of Liquid-Liquid Mixing in T-shaped Micro-Mixers using  $\mu$ -LIF and  $\mu$ -PIV. *Chemical Engineering Science*. 61: 2968-2976.
- [14] Eichhorn, Smalls. 1964. Experiments on The Lift and Drag of Spheres Suspended in A Poiseuille Flow. *Journal Fluid Mechanics*. 20: 513-527.
- [15] Jeffrey, C., Pearson, A. 1965. Particle Motion in Laminar Vertical Tube Flow. *Journal Fluid Mechanics*. 22: 721-735.
- [16] Chun, B., Ladd, C. 2006. Inertial Migration of Neutrally Buoyant Particles in A Square Duct: An Investigation of Multiple Equilibrium Positions. *Physics of Fluids*. 18: 03170.
- [17] Kim, W., Yo, Y. 2008. The Lateral Migration of Neutrally-Buoyant Spheres Transported through Square Microchannels. *Journal of Micromechanics and Microengineering*. 18: 065015.
- [18] Zheng, X., Silber-Li, H. 2009. The Influence of Saffman Lift Force on Nanoparticle Concentration Distribution near a Wall. *Applied Physics Letter*. 95: 124105.
- [19] Griffiths, H., Tucker, G., Sage, I., Hrenden-Harker, G. 1996. An Electrical Impedance Tomography Microscope. *Physiology Measurement*. 17: 15-24.
- [20] York, A., Phua, N., Reichelt, L., Pawlowski, A., Kneer, R. 2006. A Miniature Electrical Capacitance Tomography. *Measurement Science and Technology*. 17: 2119-2129.
- [21] Choi, J., Takei, M. 2010. Sub-Micro Particle Distribution of Measurement and Simulation in Cross-Section of Microchannel by Process Computed Tomography. *IEEE Journal*. 41-46.
- [22] Choi, J., Takei, M., Doh, H. 2010. Fabrication of Microchannel with 60 Electrodes and Capacitance Measurement. *Flow Measurement and Instrumentation*. 21: 178-183.
- [23] Ali Othman, T., Obara, H., Choi, E., Takei, M. 2011. Temporally Transitional Cross-Sectional Capacitance Measurement of Micro Particles Concentration in the Microchannel. *Japanese Journal of Multiphase Flow*. 25: 423-434.
- [24] Ali Othman, T., Obara, H., Takei, M. 2013. Cross-Sectional Capacitance Measurement of Particles Concentration in a Microchannel with Multi-Layered Electrodes. *Flow Measurement and Instrumentation*. 31: 47-54.